RSC Advances

PAPER

View Article Online
View Journal | View Issue

Cite this: *RSC Adv.*, 2020, **10**, 11325

Functionalized polyhedral oligosilsesquioxane (POSS) based composites for bone tissue engineering: synthesis, computational and biological studies†

Laura Legnani,[a] Daniela Iannazzo,[b] Alessandro Pistone,[b] Consuelo Celesti,[b] Salvatore Giofrè,[c] Roberto Romeo,[c] Angela Di Pietro,[d] Giuseppa Visalli,[d] Monica Fresta,[a] Paola Bottino,[a] Ignazio Blanco[e] and Maria Assunta Chiacchio *[a]

Received 20th February 2020
Accepted 12th March 2020

DOI: 10.1039/d0ra01636e

rsc.li/rsc-advances

Functionalized polyhedral oligosilsesquioxanes (POSS) containing an isoxazolidine nucleus have been synthesized by microwave assisted 1,3-dipolar cycloaddition of *N*-methyl-*C*-alkoxycarbonyl nitrone **1** with POSS containing olefin moieties. The results of cycloaddition processes were rationalized by computational studies at the DFT level. The covalent conjugation of chitosan with the cycloadduct **3a** leads to composite material CS-POSS **7** which was gelified using genipin as cross linking agent. The suitability of the system for bone tissue engineering purposes was evaluated by *in vitro* drug release studies using ketoprofen as a model drug and cytotoxicity assays performed on human fetal osteoblastic cells. The preliminary biological tests showed the lack of cytotoxicity of the hybrid material and suggest its potential role in bone tissue engineering applications.

1. Introduction

Biopolymer-based composites containing inorganic materials with inherent bioactive properties and cytocompatibility have attracted significant interest in tissue engineering, leading to the development of bone scaffolds to be used both as bone grafts and drug delivery systems.[1,2] These biomaterials have shown the ability to promote damaged tissue repair and regeneration by intrinsic osteoinductive properties and/or by triggering stimulating effects on bone cells and tissues, such as pH, ionic strength, temperature, light and magnetic fields.[3] The main advantage in using hybrid materials lies in their ability to mimic the composite structure of natural bone and teeth which are mainly constituted of an organic phase, collagen type 1, and an inorganic component, hydroxyapatite.[4] Ideal composites for tissue engineering applications should be biocompatible, able to mimic and interact with the natural environment of extracellular matrix (ECM), and possess suitable mechanical properties to provide support for the newly formed tissue and also to withstand external forces during bone tissue regeneration.[5]

Several fabrication techniques have been used to develop bone tissue engineering scaffolds, using a wide range of biomaterials whose choice mainly depends on the site of implantation for which the scaffold is designed. Three-dimensional scaffolds constituted by natural polymeric biomaterials including proteins and polysaccharides, have shown to provide ideal structural support and to allow a suitable environment for cell adhesion, migration, proliferation and differentiation.[6]

Among the different polysaccharide-based 3D scaffolds, the naturally derived polymers such as chitin, chitosan, collagen, gelatin, alginate, hyaluronic acid and their composites, due to their high biocompatibility, biodegradability, low cost, ease of handling, and possibility of gelation *in situ*, represent resourceful biomaterials for bone and soft tissue engineering applications.[7] Moreover, these biopolymers can be cross-linked, allowing the incorporation of cells, growth factors and the controlled release of bioactive molecules.[8] Among the different investigated biopolymers, the natural polysaccharide, chitosan (CS), obtained from the deacetylation of chitin, due to its good biocompatibility, biodegradability, ease of chemical modifications, antibacterial properties and high affinity *in vivo* with macromolecules represent an ideal organic material for the development of biopolymer based scaffold for organ and tissue regeneration.[9,10] However, besides its outstanding chemical,

[a]*Dipartimento di Scienze del Farmaco, Università di Catania, Viale A. Doria 6, 95125 Catania, Italy. E-mail: ma.chiacchio@unict.it*

[b]*Dipartimento di Ingegneria, Università di Messina, Contrada Di Dio, 98166 Messina, Italy*

[c]*Dipartimento di Scienze Chimiche, Biologiche, Farmaceutiche ed Ambientali, Università di Messina, Via S.S. Annunziata, 98168 Messina, Italy*

[d]*Dipartimento di Scienze Biomediche, Odontoiatriche e delle Immagini Morfologiche e Funzionali, Via Consolare Valeria 1, 98100, Messina, Italy*

[e]*Dipartimento di Ingegneria Civile e Architettura, Università di Catania, Viale A. Doria 6, 95125 Catania, Italy*

† Electronic supplementary information (ESI) available. See DOI: 10.1039/d0ra01636e

physical and biological features, the applications of scaffolds based on this natural polysaccharide show some limitations mainly related to its low mechanical strength, quick hydrolysis and burst drug release which limit its use, as single component, in bone tissue engineering formulations.[11,12]

In order to improve the mechanical behavior and biological stability of chitosan based scaffolds the 3D hydrogels have been reinforced with bioactive ceramic materials such as hydroxyapatite (HA), bioglass ceramic, silica nanoparticles, titanium dioxide and zirconium oxide.[13–15] Among the different inorganic compounds, silica nanoparticles have shown to improve mechanical properties of polymers by providing enhancement in their structure and increasing the bioactivity of the related composites. Moreover, a recent *in vitro* study demonstrated the ability of silicate-based bioactive glasses to induce calcium hydroxy-carbonate apatite on the silica surface, with a close composition to bone mineral composition.[16]

The polyhedral oligomeric silsesquioxanes (POSS) are silicon/oxygen cage structures with $RSiO_{3/2}$ repeat units and size range of 1–3 nm. These compounds are characterized by a hybrid chemical composition, intermediate between that of inorganic materials (SiO_2) and organic silicone polymers (R_2SiO).[17] This structural peculiarity confers to POSS, "hybrid" properties and then the ability to be inert and thermally stable due to the presence of the inorganic Si–O–Si fragment and also the reactivity and ability to be readily modified because of the presence of R–Si fragment. Due to their nanoscale dimensions and the possibility to form stable covalent and non covalent interactions with organic polymers, several POSS containing composites have been developed for applications in different materials areas such as the development of bio-polymers, high-temperature composites, liquid crystals, and coatings for spacecraft.[17,18] In particular, POSS silica cages, due to their biocompatibility and physico-chemical properties, able to enhance the mechanical and rheological properties of biopolymers, have shown to be suitable nanofillers for a wide range of composites for biomedical applications, thus leading to the development of biomedical devices, tissue engineering scaffolds, drug delivery systems, and biosensors.[19–21] In addition, it was proved that these nanostructured materials can stimulate important biological responses at nanoscopic dimensions, such as cell adhesion and apatite formation.[22,23]

In this study, we exploited the useful functionalization of cubic silsesquioxanes with $(RSiO_{3/2})_8$ formula in order to afford POSS substrates containing suitable functional groups able to form a covalent bond with the chitosan structure. The insertion of a reactive olefin moiety[24] at the organic side chain (group R) of heptaisobutyl-POSS, allowed the effective microwave assisted 1,3-dipolar cycloaddition reaction with the *N*-methyl-*C*-alkoxycarbonyl nitrone **1**, affording the corresponding isoxazole derivatives **3a,b**, **4a,b** and **5b**, containing an ethoxycarbonyl group at the C-3 position of heterocyclic nucleus. The further amidation reaction between the ethoxycarbonyl group of the isomer formed in the greater amount **3a** and the amino group of chitosan allowed the formation of the POSS-chitosan hybrid material which was gelified using the cross-linking agent genipin, a natural compound endowed with very low toxicity.[25] The synthesized hydrogel scaffolds were investigated for their drug release abilities using ketoprofen as model drug which was included in the scaffold during the gelation procedure. The results of *in vitro* drug release studies and the preliminary biological tests performed on osteoblasts culture have shown the lack of cytotoxicity of the hybrid material, thus revealing the CS-POSS 7 as a potential candidate for bone tissue engineering applications.

2. Results and discussion

2.1. Synthesis of isoxazolidinyl-POSS 3a,b, 4a,b and 5b

The 1,3-dipolar cycloaddition reactions of allyl-**2a** and vinyl-heptaisobutyl-POSS **2b** with *N*-methyl-*C*-ethoxycarbonylnitrone **1**, were performed under microwave irradiation at the temperature of 100–110 °C in 90 min, following a previously reported procedure.[26] The pericyclic reaction with allyl-heptaisobutyl-POSS **2a** leads to the formation of two cycloadducts: **3a** and **4a**, with no formation of other regioisomers **5a** and **6a**. The reaction showed a very good control of regio- and stereoselectivity with the *trans* isomer **3a** as the main adduct with a relative ratio *trans*/*cis* **3a**/**4a** of 5.7 : 1 (Scheme 1).

The structure and regiochemistry of the obtained compounds were assigned on the basis of the spectroscopic data. In particular, the ^{1}H NMR spectra of **3a** shows the presence of the diagnostic methine proton at C-5 as multiplet at 4.27–4.21 ppm, the H-3 signal as a doublet of doublet centered at 3.27 ppm, while the H-4 protons resonate as doublet of triplet at 2.58 ppm and as doublets of doublets of doublets at 2.15 ppm. The stereoisomer **4a** shows the H-5 proton as a doublet of triplet of doublets centered at 4.39 ppm, the H-3 proton as triplet centered at 3.51 δ, and the H-4 protons at 2.68 and 2.22 ppm as doublets of doublets of doublets. The ^{29}Si NMR spectrum shows the signal of the O–Si–CH_2–isoxazolidine group at −67.68 ppm and the signal of –O–Si–$CH_2CH(CH_3)_2$ units at −67.97 ppm (see ESI†).

The stereochemical assignment of compounds **3a** and **4a** were obtained by NOE experiments. A positive NOE effect was registered for the *trans* compound **3a** between the H_5 and the upfield H_{4a} protons while for the compound **4a** the positive NOE

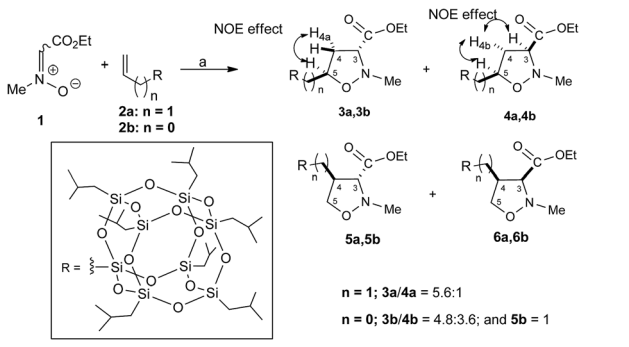

Scheme 1 Synthesis of isoxazolidinyl-POSS **3a**, **4a**, **3b**, **4b** and **5b**. Reagents and conditions: toluene, 100 W, 110 °C, 90 min. [(**3a**: 85%; **4a**: 15% yield); (**3b**: 48.0%, **4b**: 36.0% and **5b**: 10.0% yield)].

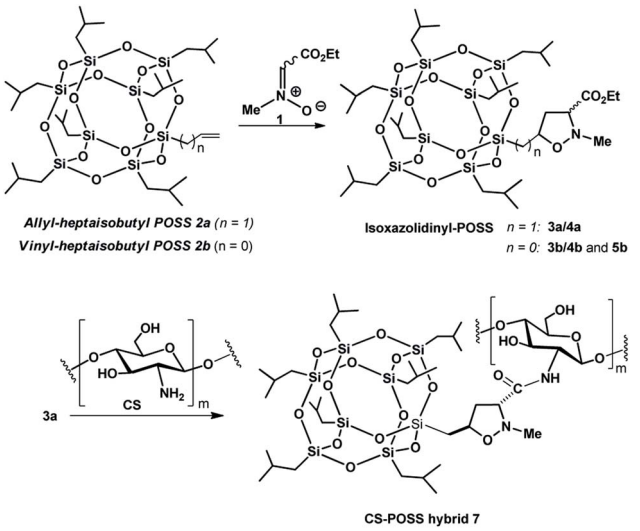

Fig. 1 Synthesis of CS-POSS hybrid **7**.

effect between H_5, H_3 and H_{4b} protons are indicative of a topological *cis* relationship.

The 1,3-dipolar cycloaddition reaction of vinyl-heptaisobutyl-POSS **2b** performed in the same reaction conditions used for **2a** afforded a mixture of **3b**, **4b** and **5b** in a 1.5 : 1.4 : 1 relative ratio with no formation of the **6b** (Scheme 1). The appearance of the regioisomer **5b** in the reaction mixture between **1** and **2b** was easily deduced from the ^{1}H NMR spectrum which presents the H-5 protons as doublets of doublets at 4.11 and 3.99 ppm, respectively.

The stereochemical assignment of compounds **3b**, **4b** and **5b** were obtained by NOE experiments. Thus, a positive NOE effect was registered for the *trans* compound **3b** between the H-5 and the upfield H_{4a} protons while for the compound **4b** the positive NOE effect between H-5, H-3 and H_{4b} protons are indicative of a topological *cis* relationship. For the compound **5b**, no NOE effect was registered between H-3 and H-4 protons indicating a relative topological *trans* relationship.

2.2. Theoretical calculations

In order to rationalize the regio- and stereoselectivity of the reaction, considering the different dipolarophile reactivity of the POSS-substituted olefin **2a,b** with nitrone **1**, a mechanistic study of the cycloaddition process was done using DFT calculations.[27]

Calculations were performed using the Gaussian 16 program package.[28] All the structures were optimized at the B3LYP/6-31G(d) level. Vibrational frequencies were computed at the same level of theory to define the optimized structures as minima or transition states.

Starting from the nitrone **1** *E* or *Z* and taking into account the possible *exo* or *endo* approach of the dipolarophiles for the two possible regioisomers, eight different transition states (TSs) were supposed. In Fig. 2 are reported the possible TSs, giving, for each nitrone's isomer, the stereoisomeric products 3–6, with the groups POSS and $-CO_2Et$ in *cis* or *trans*, respectively.

Considering the cycloaddition, involving the heptaisobutyl-1-allyl-POSS **2a**, in Fig. 3 are reported the three-dimensional plots of the TSs leading to the cycloadducts **3a** and **4a** (TSs of compounds **5a** and **6a** are reported in ESI†). The activation energy and free energy values at 383 K are given in Table 1. The TS **3a**_*E*/*Z* are favorites with $\Delta G^{\ddagger}$ of 26.20 and 28.16 kcal mol^{-1}, which produce 95% yield of *trans* adduct **3a**. The TS **4a**_*E*/*Z* ($\Delta G^{\ddagger}$ 29.60/30.64 kcal mol^{-1}), is higher in energy and gives 3.1% yield of the *cis* derivative **4a**. As regard to the regioisomer **5a**, the lower TS (TS_**5a**_*E*) for its formation has a $\Delta G^{\ddagger}$ of 31.40 kcal mol^{-1} and leads to the formation of 2% yield of this cycloadduct but, having an energy barrier more than 30 kcal mol^{-1}, the cycloaddition does not occur. Furthermore, the TS energies of **6a** (TS_**6a**_*E* and TS_**6a**_*Z*) are too high, thus, this compound can't be obtained in this cycloaddition process.

Both C–C and C–O bonds are formed in a concerted albeit asynchronous way, as evident by distances between atoms involved in the forming bonds (Å) reported in the 3D plots. The pathway leading to regioisomers **5a** and **6a** (see ESI†) resulted to be more asynchronous respect to that leading to regioisomers

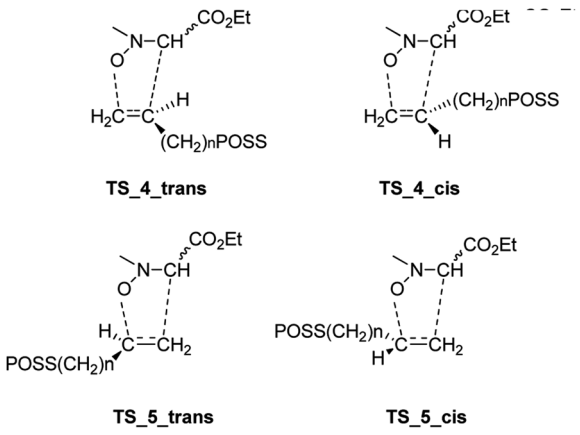

Fig. 2 Possible TSs of the cycloaddition of nitrone **1** with dipolarophiles **2a**,**b**.

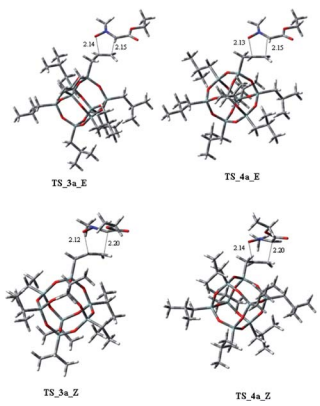

Fig. 3 Transition states for **2a** with **1** leading to stereoisomers **3a**, **4a**. Displacement vectors for TS imaginary frequencies are shown as grey arrows and the values of the forming bond lengths are reported in angstroms.

Table 1 Activation energies and free energies *in vacuo* of cycloaddition of heptaisobutyl-1-allyl-POSS **2a** with **1**

TSs	$\Delta E^{\ddagger}$ (kcal mol^{-1})	$\Delta G^{\ddagger}$ (kcal mol^{-1})	% (T = 383 K)
TS_**3a**_*E*	13.14	26.20	78.7
TS_**4a**_*E*	15.15	29.60	5.5
TS_**5a**_*E*	15.51	31.40	3.4
TS_**6a**_*E*	17.03	34.23	0.5
TS_**3a**_*Z*	14.38	28.16	11.2
TS_**4a**_*Z*	16.92	30.64	0.4
TS_**5a**_*Z*	17.97	33.48	0.1
TS_**6a**_*Z*	17.75	34.15	0.1

3a and **4a**; anyway, both processes are concerted, as confirmed by IRC analysis.

On the other hand, considering the cycloaddition of **2b** with **1** in Fig. 4 and 5 are reported the three-dimensional plots of the transition states to the regioisomeric cycloadducts **3b–6b** and in Table 2 the activation energy, the free energy values and the percentages at 383 K.

In this case, the ratio of the two regioisomers **3b**/**4b** *vs.* **5b** is 8.4 : 1, according with experimental data. The *trans*/*cis* ratio in **3b** *vs.* **4b** is 4.8 : 3.6. It is worth to note that the TSs **5b**_*E*, and **5b**_*Z*, leading to **5b** have $\Delta G^{\ddagger}$ of 28.73 and 29.94 kcal mol^{-1}, clearly lower of the corresponding regioisomer **5a** (**5a**_*E*, **5a**_*Z*: 31.40/33.48 kcal mol^{-1}). Thus, these results could justify the preferred formation of **5b** with respect to **5a**. As observed for the cycloaddition reaction of **2a**, also for **2b**, the IRC analyses allowed us to verify that the reaction is concerted, albeit slightly asynchronous (Fig. 4 and 5). In conclusion, the modeling study, according to the experimental results, rationalized that the 1,3-dipolar cycloaddition of **1** with **2a** or **2b** is regio- and stereoselective.

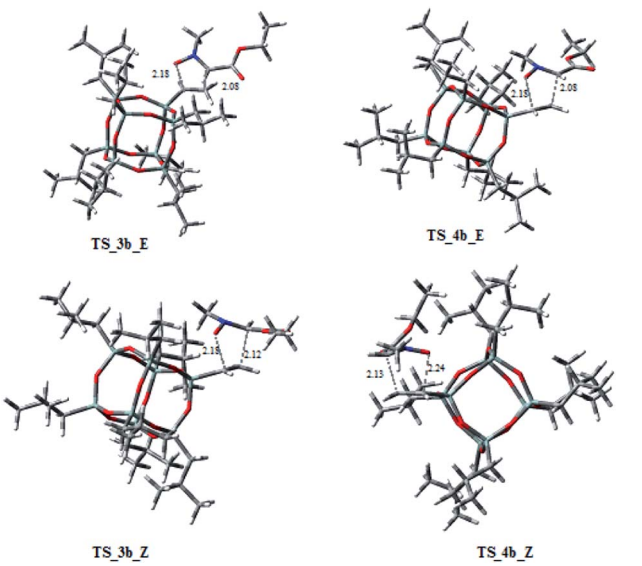

Fig. 4 Transition states for the reaction of **2b** with **1** leading to stereoisomers **3b** and **4b**. Displacement vectors for TS imaginary frequencies are shown as grey arrows and the values of the forming bond lengths are reported in angstroms.

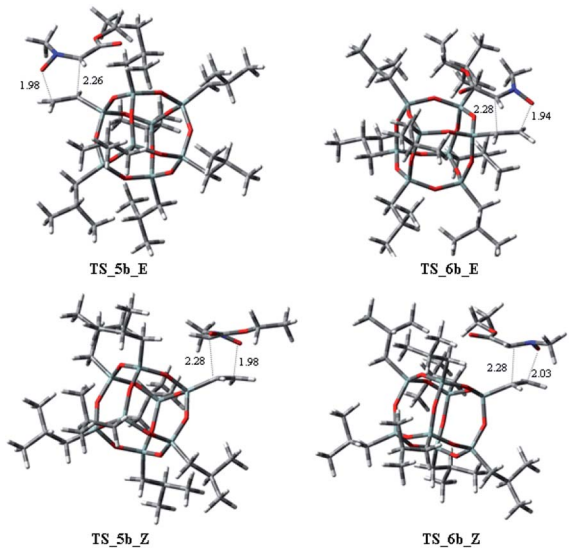

Fig. 5 Transition states for the reaction of **2b** with **1** leading to stereoisomers **5b** and **6b**. Displacement vectors for TS imaginary frequencies are shown as grey arrows and the values of the forming bond lengths are reported in angstroms.

2.3. Synthesis of CS-POSS hybrid hydrogels

The main isomer **3a** obtained from the 1,3-dipolar cycloaddition of **2a** with nitrone **1** was used for the *tert*-butoxide-assisted amidation reaction with the free nucleophilic amino group of chitosan.[29] The reaction led to the formation of the hybrid sample CS-POSS 7 (Fig. 1). In order to achieve the complete amidation of **3a**, the reaction was performed using an excess of biopolymer (see Experimental section). The effectiveness of the coupling reaction between **3a** and chitosan was investigated by FTIR spectroscopy and TGA analysis. The FTIR spectra of CS-POSS 7, compared with those of precursors chitosan (CS) and of POSS cycloadduct **3a** is reported in Fig. 6. The spectrum of CS shows a strong band at 3150–3600 cm^{-1} corresponding to the stretching of N–H and O–H bonds, the peaks at 2850 and 2920 cm^{-1} due to the aliphatic C–H stretching, a band at 1575 cm^{-1} ascribable to the N–H bending, a peak at 1030 cm^{-1}

Table 2 Activation energies and free energies *in vacuo* of cycloaddition of heptaisobutyl-1-vinyl-POSS **2b** with **1**

TSs	$\Delta E^{\ddagger}$ (kcal mol^{-1})	$\Delta G^{\ddagger}$ (kcal mol^{-1})	% (T = 383 K)
TS_**3b**_*E*	12.23	27.86	36.1
TS_**4b**_*E*	12.86	28.36	15.7
TS_**5b**_*E*	12.95	28.73	0.4
TS_**6b**_*E*	12.60	30.84	1.8
TS_**3b**_*Z*	15.40	31.64	13.9
TS_**4b**_*Z*	14.26	28.96	22.2
TS_**5b**_*Z*	13.01	29.94	9.4
TS_**6b**_*Z*	15.27	32.86	0.5

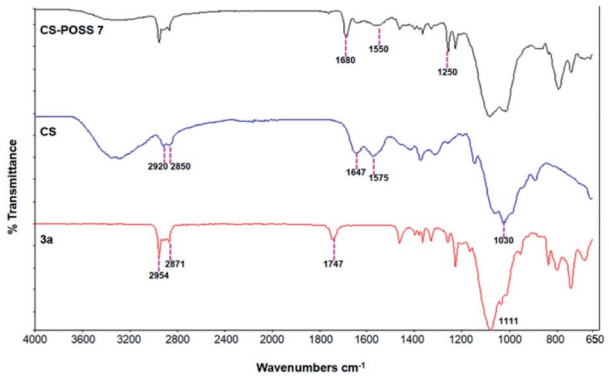

Fig. 6 FTIR spectra of samples **3a**, CS, and CS-POSS **7**.

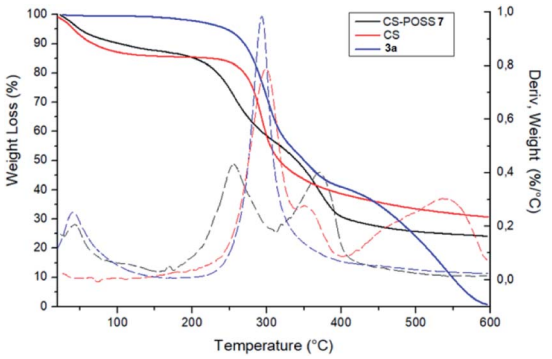

Fig. 7 TGA thermograms of CS-POSS 7, CS and of compound **3a** performed under nitrogen atmosphere.

corresponding to the C–O stretching and a peak at 1647 cm^{-1} due to the C=O stretching of the primary amide of residual *N*-acetyl groups. Compound **3a** shows the diagnostic signals at 1111 cm^{-1} ascribable to the Si–O–Si stretching of silica cage, the aliphatic C–H stretching of isobutyl substituents at 2954 cm^{-1} and 2871 cm^{-1} and the presence of a peak at 1747 cm^{-1} due to the C=O stretching of the ester group present at C-3 position of the isoxazolidine nucleus. The hybrid sample CS-POSS 7 shows the presence of the diagnostic peak at 1680 cm^{-1} attributable to the C=O stretching of the newly formed amide bond, the presence of a peak at 1550 cm^{-1} ascribable to the N–O stretching and a peak at 1250 cm^{-1} due to the absorbance of the C–N bond; moreover a large band at 3100–3600 cm^{-1} lower in intensity with respect to CS sample, can be observed.

The covalent conjugation of chitosan with **3a** that leads to CS-POSS 7 was also confirmed by thermogravimetric analysis (TGA) performed under nitrogen environment (Fig. 7). The thermal degradation of pure chitosan shows two stages in the range of 50–400 °C. The first (range 50–100 °C) is due to the loss of water with a weight loss of about 9%, while the second stage (range 250–400 °C) shows a complete degradation of the sample with a maximum decomposition temperature at 300 °C and a total weight loss of about 70%. The POSS cycloadduct **3a** shows the initial thermal decomposition temperature at 235 °C, a maximum decomposition temperature at 293 °C and a complete thermal degradation at 600 °C. The TGA curve of the hybrid material CS-POSS 7 shows a different profile with respect to precursors chitosan and **3a**. For this sample, three different degradation stages can be observed: the first at 50–100 °C attributable to the loss of water, the second at 190–300 °C with a maximum decomposition at 254 °C and the third at 300–400 °C with a maximum decomposition temperature at 371 °C and a complete degradation of the sample with a total weight loss of about 75%. The different degradation temperatures and the different shape of TGA curves are indicative of the formation of a new composite material with a different thermal behavior with respect to precursors CS and **3a**.

Furthermore, the ^{29}Si NMR spectrum of CS-POSS 7 performed in $CDCl_3$ (see ESI†) confirms that under our reaction conditions, the cage of the POSS remains intact. In fact, only two signals appeared at −67.65 and −67.96, corresponding to Si–CH_2–isoxazolidine and to Si–CH_2–$CH(CH_3)_2$, respectively.

The synthesized CS-POSS 7 and pure chitosan were gelified using the natural and biocompatible cross-linking agent genipin in order to compare the drug release properties of the formed hydrogels. The gelification process was performed in the presence of an aqueous solution of the anti-inflammatory drug ketoprofen (80 mg mL^{-1}) at the concentration of 4 wt% with respect to the weight of biopolymers-based samples. Since genipin cross-links macromolecules by binding two amine groups between neighboring chains, the CS-POSS 7, because of the steric hindrance caused by POSS molecule bonded to chitosan chains, showed a more delayed gelation time with respect to the hydrogel obtained from unmodified chitosan (Scheme 2).

Compared to the CS hydrogel, the introduction of POSS molecule in the CS-POSS 7 hydrogel, have shown to decrease the water penetration, due probably to the different cross-linking ability and to the presence of hydrophobic components. In fact, the amount of water, evaluated as difference between the weight of composite before and after drying, was found to be of 94 wt% and 78 wt% for CS and CS-POSS 7 hydrogels, respectively.

The rheological properties of the synthesized chitosan-based hydrogels were evaluated by measuring the storage modulus (G') and the loss modulus (G''), as a function of frequency range from 10^{-1} Hz to 10 Hz (See ESI†). The results of these studies demonstrated, for both hydrogels, G' values higher than the G'' value, thus indicating an elastic solid behaviour. Moreover, higher G' and G'' values have been found for CS-POSS 7 sample, revealing for this hybrid material, an increased stiffness with respect to the pure CS hydrogel. These results are in complete agreement to what reported in literature for hydrogels containing POSS molecules.[18,21]

2.4. Drug release studies

The drug release behaviour was evaluated from the hydrogels obtained from CS and CS-POSS 7, in order to investigate the effect of the presence of the silica cage on the drug release properties of the chitosan-based matrices. The study was performed at the normal body temperature of 37 °C, in buffer phosphate solution (pH = 7.4) using the dialysis bag diffusion

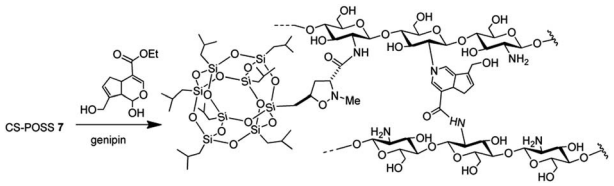

Scheme 2 Cross-linking reaction of CS-POSS 7 with genipin (see Experimental details).

technique and in an orbital shaker rotating at 30 rpm. The amount of drug released was quantified by UV-Vis absorption spectra, by measuring the drug absorbance at 260 nm (Fig. 8). The hydrogel obtained from CS shows a burst drug release (about 65%) within 1 hour that reached 100% of drug released within 1 day. For the hydrogel obtained from CS-POSS 7 the release curve showed also a fast release of great amounts of ketoprofen (45%) in the first hour but a more controlled release in the next two days, reaching a plateau at about 78% of ketoprofen loaded. The results on this study suggest the presence of specific intermolecular interactions between the functionalized silica cage and the drug and open new possibilities for a long term sustained release of drugs entrapped inside the polymeric matrix during its *in vivo* biodegradation.

2.5. Cell cultures and biological assays

Human fetal osteoblastic cells (hFOB 1.19) were used as *in vitro* model to evaluate the cytotoxicity of the synthesized CS and CS-POSS 7 hydrogels. Both samples were gelified at room temperature and the cells were plated and grown on the formed hydrogels for 48 h at 34 °C in an atmosphere of 5% CO_2 in order to simulate the natural living tissue environment. Cells cultured in their specific medium, were used as negative controls.

Cytotoxicity studies have shown that the investigated hydrogels, as evaluated using the DNA intercalating probe propidium iodine (PI) and by fluorimetric analysis (λ_{exc} 493–λ_{em} 636 nm)

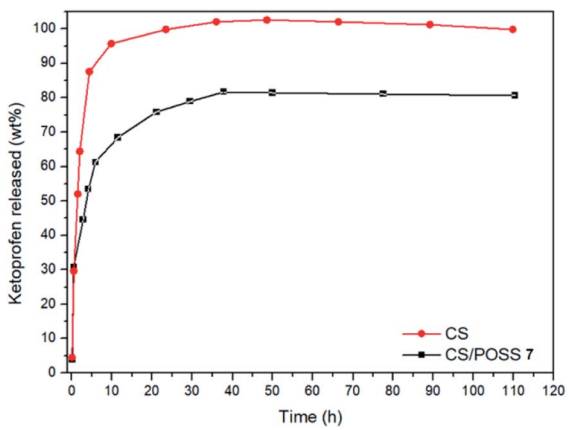

Fig. 8 Ketoprofen release from CS and CS-POSS 7 hydrogels at 37 °C, in PBS (pH 7.4).

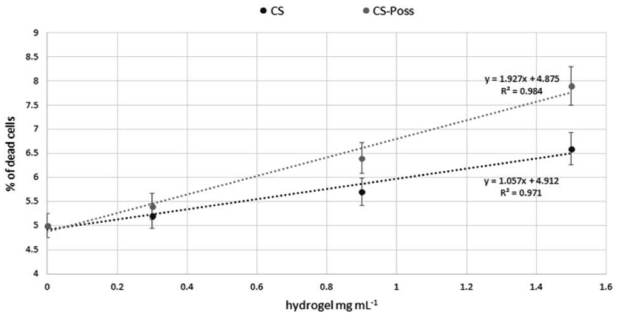

Fig. 9 Percentages of dead cells grown in presence of CS and CS-POSS 7 hydrogels.

were not cytotoxic to osteoblasts. At the lowest dose tested, the percentages of dead cells were superimposable with control cells (5% ± 0.3 *vs.* 5.2 ± 0.4 and 5.4 ± 0.6 CS and CS-POSS 7 hydrogels respectively). As shown in Fig. 9, a very limited increase in the mortality rates was observed at the highest doses, highlighting the low cytotoxicity of both hydrogels. In particular, compared to highly biocompatible CS, the hybrid material increased the percentages of dead cells on average by 12%.

In addition, the use of acridine orange (AO), a cell-permeable, nucleic acid-selective fluorescent cationic dye, allowed the analysis of cell compartments. The Confocal Laser Scanning Microscope, (CLSM) images confirmed that the cells grown in presence of the hydrogels were morphologically analogous to controls (Fig. 10).

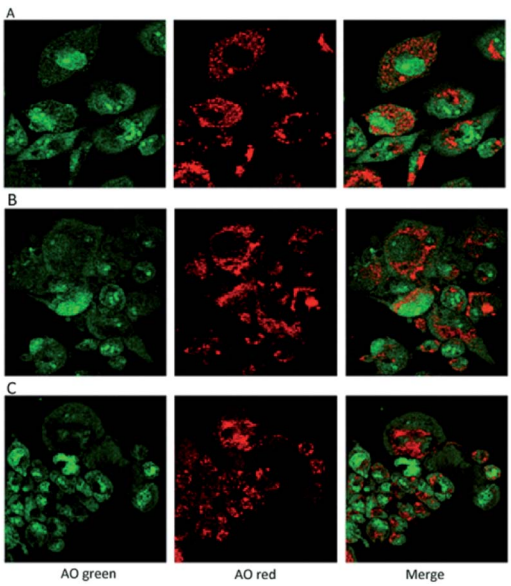

Fig. 10 CLSM images of hFOB 1.19 cells labelled with the metachromatic fluorophore AO. (A) Control cells; (B) osteoblastic cells grown in presence of CS hydrogel; (C) osteoblastic cells grown in presence of CS-POSS 7 hydrogel. In the nucleus the AO, intercalating with DNA emits a green florescence while in the cytosol, the fluorophore is sequestered in the intact lysosomes where, due to the low pH, it becomes protonated and emits a red florescence. In presence of acid compartment damage only green florescence is emitted.

3. Conclusions

We have exploited the useful functionalization of POSS silica cage to afford substrates containing functional groups suitable for the covalent bonding with the chitosan structure. The microwave assisted 1,3-dipolar cycloaddition of POSS derivatives containing olefin moieties, with the *N*-methyl-*C*-alkoxycarbonyl nitrone afforded the corresponding isoxazolidine derivatives containing an ethoxycarbonyl group at the C-3 position of heterocyclic nucleus. Theoretical calculations confirmed the experimental observations leading to C-5 substituted derivatives as preferred cycloadducts. Furthermore, the relevant formation of compound **5b** in the case of cycloaddition of **1** with vinyl-POSS **2b** can be rationalized by $\Delta G^{\ddagger}$ energies of the corresponding TSs and by the shorter distance of the incoming C–O bond in the transition state with respect to what observed for the cycloaddition of allyl-POSS **2a**.

The amidation reaction between the amino group of chitosan and the ethoxycarbonyl group of the major isomer **3a**, allowed the formation of the hybrid material CS-POSS 7 which was gelified using the cross-linking agent genipin. The synthesized hydrogel scaffold was investigated for its ability to release ketoprofen, which was included in the scaffold during the gelation procedure. *In vitro* drug release studies and preliminary biological tests performed on osteoblasts culture, have shown the ability of the system to release drugs in a controlled manner and the lack of cytotoxicity of the hybrid material. Thus, the results of this work highlight the sample CS-POSS 7 as a potential candidate for bone tissue engineering applications.

4. Experimental section

4.1. Materials and methods

Solvents, allyl-heptaisobutyl-POSS **2a** and vinyl-heptaisobutyl POSS **2b** and other chemical reagents were purchased from Sigma-Aldrich and were used without further purification. The reactions under microwave irradiations were carried out using a CEM Corporation Focused Microwave System, Model Discover. Thin-layer chromatographic separations were carried out on Merck silica gel 60-F254 precoated aluminum plates (Merck, Darmstadt, Germany). Flash chromatography was carried out using Merck silica gel (200–400 mesh). Preparative separations were carried out using a Büchi C-601 MPLC instrument (BUCHI Italia S.r.l., Milano, Italy) using Merck silica gel 0.040–0.063 mm, and the eluting solvents were delivered by a pump at the flow rate of 3.5–7.0 mL min^{-1}. NMR spectra were recorded on a Varian Unity Inova instrument (^1H at 500 MHz, ^{13}C at 125.67 MHz, ^{29}Si at 99.32 MHz). Chemical shifts are in ppm (δ) using TMS as internal standard. NOE difference spectra were obtained by subtracting alternatively right-off-resonance free induction decays (FIDS) from right-on-resonance-induced FIDS. Thermogravimetric analyses (TGA) were performed using a TAQ500 instrument (TA Instruments, New Castle, DE, USA) from 100 to 700 °C, with a rate of 20 °C per minute, under air atmosphere. The Infrared spectra were obtained using the Fourier-Transform Infrared (FT-IR) spectrometer VERTEX 80/80v (Bruker Optik GmbH, Ettlingen, Germany), by the method of KBr pellets in the range of 4000–500 cm^{-1}. UV spectra have been performed by Thermo Nicolet mod, Evolution 500 spectrophotometer, measuring the drug absorbance at 260 nm. Rheological properties measurements were carried out on a rotational Rheometer (Mod. SR5, Rheometric Scientific) with parallel plate geometry at 37 °C; cylindrical samples had a diameter of 25 mm and a height of 1 mm. Storage and loss modulus were measured by using a frequency sweep mode with the range from 0.1 to 10 Hz (rad s^{-1}). Cell line hFOB 1.19 was purchased from Izsler (Istituto Zooprofilattico "B. Ubertini" Brescia, Italia), cell culture media and fluorophores were purchased from Sigma-Aldrich. Fluorimetric analyzes were performed by a microtiter plate reader (Tecan Italia, Milan-Italy) while a TCS SP2 (Leica Microsystems, Heidelberg, Germany), equipped with Ar/Kr laser and coupled to a microscope (Leica DM IRB) was used for morphological analyses.

4.2. General procedure

4.2.1 Synthesis of isoxazolidinyl-POSS 3a,b, 4a,b and 5b. A mixture of nitrone **1** (200 mg, 1.52 mmol) and allyl-heptaisobutyl POSS (132 mg, 0.15 mmol) **2a** or vinyl-heptaisobutyl-POSS (128 mg, 0.15 mmol) **2b**, dissolved in toluene (2 mL) in a pressure tube equipped with a stirrer bar, was inserted into the cavity of a Discover Microwave System apparatus and heated for 90 min at 100 W at the internal temperature of 100–110 °C. The mixture was then evaporated and the resulting solid was purified by flash chromatography on silica gel using cyclohexane/ethyl acetate (80 : 20) as eluent, to afford isoxazolidines **3a**, **4a** from allyl-heptaisobutyl POSS **2a** and isoxazolidines **3b**, **4b** and **5b** from vinyl-heptaisobutyl-POSS **2b**.

*4.2.1.1. Reaction of nitrone **1** with allyl-heptaisobutyl POSS **2a**.* The first eluted product was ethyl(3*RS*,5*RS*)-5-(3,5,7,9,11,13,15-heptaisobutylpentacyclo[9.5.1.1^{3,9}.1^{5,15}.1^{7,13}]octasilox-1-yl)-2-methylisoxazolidine-3-carboxylate (**3a**) (85%, 170 mg), sticky white solid, δ ^1H (500 MHz, $CDCl_3$) 4.28–4.19 (m, 3H, O–CH_2–, and H_5), 3.27 (dd, 1H, J = 6.5, 9.9 Hz, H_3), 2.79 (s, 1H, N–CH_3), 2.58 (dt, 1H, J = 12.4, 6.5 Hz, H_{4b}), 2.15 (ddd, 1H, J = 12.4, 9.9, 8.1 Hz, H_{4a}), 1.93–1.78 (m, 7H, CH isobutyl), 1.29 (t, 3H, J = 7.1 Hz, $-CH_2-\underline{CH_3}$), 0.96 (d, 21H, J = 1.4 Hz, CH_3 isobutyl), 0.95 (d, 21H, J = 1.3 Hz, CH_3 isobutyl), 0.94–0.81 (m, 2H, –CH_2–Si), 0.60 (d, 14H, J = 7.2 Hz, CH_2 isobutyl). δ ^{13}C (125 MHz, $CDCl_3$) 170.87, 74.05, 70.07, 61.32, 40.64, 29.86, 25.84, 24.01, 22.62, 22.56, 18.52, 14.30. δ ^{29}Si NMR (99.32 MHz, $CDCl_3$) −67.68 and −66.97. Anal. calcd for $C_{37}H_{79}NO_{15}Si_8$: C, 44.32; H, 7.94; N, 1.40. Found: C, 44.30; H, 7.95; N, 1.39.

The second eluted product was ethyl(3*SR*,5*RS*)-5-(3,5,7,9,11,13,15-heptaisobutylpentacyclo[9.5.1.1^{3,9}.1^{5,15}.1^{7,13}]octasilox-1-yl)-2-methylisoxazolidine-3-carboxylate (**4a**) (15%, 30 mg), sticky white solid, δ ^1H (500 MHz, $CDCl_3$) 4.39 (dtd, 1H, J = 10.9, 7.2, 3.7 Hz, H_5), 4.21 (q, 2H, J = 7.0 Hz, O–CH_2–), 3.51 (t, 1H, J = 7.6 Hz, H_3), 2.75 (s, 3H, N–CH_3), 2.68 (ddd, 1H, J = 12.6, 8.5, 6.9 Hz, H_{4b}), 2.22 (ddd, 1H, J = 12.6, 7.6, 6.7 Hz, H_{4a}), 1.91–1.78 (m, 7H, CH isobutyl), 1.29 (t, 3H, J = 7.0 Hz, $-CH_2-\underline{CH_3}$), 1.10–1.03 (m, 2H, –CH_2–Si), 0.96 (d, 21H, J = 1.3 Hz, CH_3 isobutyl), 0.95 (d, 21H, J = 1.3 Hz, CH_3 isobutyl), 0.60 (d, 14H, J = 7.0 Hz, CH_2 isobutyl). δ ^{13}C (125 MHz, $CDCl_3$) 171.34, 73.26, 61.39, 39.76, 29.85, 25.85, 25.83, 25.80,

24.02, 24.00, 22.61, 22.56, 18.60, 14.33. Anal. calcd for $C_{37}H_{79}NO_{15}Si_8$: C, 44.32; H, 7.94; N, 1.40. Found: C, 44.35; H, 7.96; N, 1.42.

*4.2.1.2. Reaction of nitrone **1** with vinyl-heptaisobutyl POSS **2b**.* The first eluted product was (3*RS*,5*SR*)-ethyl 5-(3,5,7,9,11,13,15-heptaisobutyl-2,4,6,8,10,12,14,16,17,18,19,20-dodecaoxa-1,3,5,7,9,11,13,15-octasilapentacyclo[9.5.1.1^{3,9}.1^{5,15}.1^{7,13}]icosan-1-yl)-2-methylisoxazolidine-3-carboxylate (**3b**) (48%, 60 mg), white solid, mp: 113–115 °C. δ ^{1}H (500 MHz, $CDCl_3$) 4.22 (q, J = 7.1 Hz, 2H, O–CH_2–), 3.66 (td, J = 9.4, 1.7 Hz, 1H, H_5), 3.19 (t, J = 7.5 Hz, 1H, H_3), 2.77 (s, 3H, N–CH_3), 2.67–2.45 (m, 2H, H_4), 2.02–1.75 (m, 7H, CH isobutyl), 1.29 (t, J = 7.1 Hz, 3H, $-CH_2-\underline{CH_3}$), 0.96 (d, J = 1.4 Hz, 21H, CH_3 isobutyl), 0.95 (d, J = 1.4 Hz, 21H, CH_3 isobutyl), 0.61 (dd, J = 10.3, 7.1 Hz, 14H, CH_2 isobutyl). δ ^{13}C (125 MHz, $CDCl_3$) 171.21, 69.50, 66.37, 61.43, 36.39, 27.07, 25.85, 25.83, 24.00, 23.97, 23.96, 22.61, 22.42, 14.29. Anal. calcd for $C_{35}H_{75}NO_{15}Si_8$: C, 43.13; H, 7.76; N, 1.44. Found C, 43.16; H, 7.78; N, 1.46.

The second eluted product was (3*SR*,4*RS*)-ethyl 4-(3,5,7,9,11,13,15-heptaisobutyl-2,4,6,8,10,12,14,16,17,18,19,20-dodecaoxa-1,3,5,7,9,11,13,15-octasilapentacyclo[9.5.1.1^{3,9}.1^{5,15}.1^{7,13}]icosan-1-yl)-2-methylisoxazolidine-3-carboxylate (**5b**) (10%, 12.3 mg), white solid, mp: 93–95 °C. δ ^{1}H (500 MHz, $CDCl_3$) 4.27–4.13 (m, 2H, O–CH_2–), 4.11 (dd, J = 9.3, 8.1 Hz, H_{5b}), 3.99 (dd, J = 9.3, 8.1 Hz, 1H, H_{5a}), 3.40 (d, J = 8.5 Hz, 1H, H_3), 2.73 (s, 3H, N–CH_3), 2.35 (td, J = 9.3, 8.5 Hz, 1H H_4), 1.91–1.78 (m, 7H, CH isobutyl), 1.30 (t, J = 7.1 Hz, 3H, $-\underline{CH_2}-\underline{CH_3}$), 0.96 (d, J = 3.0 Hz, 21H, CH_3 isobutyl), 0.95 (d, J = 3.0 Hz, 21H, CH_3 isobutyl), 0.65–0.58 (m, 14H, CH_2 isobutyl). δ ^{13}C (125 MHz, $CDCl_3$) 170.96, 70.90, 67.12, 61.58, 32.02, 27.06, 25.83, 25.82, 23.98, 22.59, 22.57, 22.47, 14.27. Anal. calcd for $C_{35}H_{75}NO_{15}Si_8$: C, 43.13; H, 7.76; N, 1.44. Found C, 43.14; H, 7.77; N, 1.46.

The third eluted product was (3*RS*,5*RS*)-ethyl 5-(3,5,7,9,11,13,15-heptaisobutyl-2,4,6,8,10,12,14,16,17,18,19,20-dodecaoxa-1,3,5,7,9,11,13,15-octasilapentacyclo[9.5.1.1^{3,9}.1^{5,15}.1^{7,13}]icosan-1-yl)-2-methylisoxazolidine-3-carboxylate (**4b**) (36%, 44 mg), white solid, mp: 111–113 °C. δ ^{1}H (500 MHz, $CDCl_3$) 4.19 (q, J = 7.1 Hz, 2H, O–CH_2), 3.70 (dd, J = 12.0, 6.4 Hz, 1H, H_5), 3.46 (t, J = 7.7 Hz, 1H, H_5), 2.68 (s, 3H, N–CH_3), 2.67–2.61 (m, 1H, H_{4b}), 2.53–2.48 (td, J = 12.1, 7.1 Hz, 1H, H_{4a}), 1.93–1.79 (m, 7H, C*H* isobutyl), 1.28 (t, J = 7.1 Hz, 3H, $-\underline{CH_2}-\underline{CH_3}$), 0.95 (d, J = 1.0 Hz, 21H, CH_3 isobutyl), 0.94 (d, J = 1.0 Hz, 21H, CH_3 isobutyl), 0.67–0.56 (m, 14H, CH_2 isobutyl). δ ^{13}C (125 MHz, $CDCl_3$) 171.63, 69.42, 63.17, 61.35, 46.73, 36.85, 25.83, 25.82, 25.78, 23.99, 23.96, 23.91, 22.61, 22.36, 14.34. Anal. calcd for $C_{35}H_{75}NO_{15}Si_8$: C, 43.13; H, 7.76; N, 1.44. Found C, 43.16; H, 7.78; N, 1.45.

4.2.2 Synthesis of CS-POSS 7 hybrid. A solution of potassium *tert*-butoxide (80 mg, 0.71 mmol) in THF (5 mL, containing 0.2% of H_2O) was left under stirring in air for 1 min at room temperature. Then, compound **3a** was added to the dispersion (175 mg, 0.17 mmol) which left under stirring at r.t. for 1 h. Subsequently, a dispersion of chitosan (350 mg, medium molecular weight) in deionized water (5 mL) was added to the mixture, which was left to stir at r.t. for additional 2 h. After removal of the solvent under vacuum, the mixture was purified using a dialysis bag (MW of 12 000 Da) for 8 h. After removal of water under vacuum at 50 °C, the mixture was dried at 50 °C for 24 h at the vacuum drying pressure of 65 mbar. The sample was characterized by FTIR and TGA analysis and used for the subsequent reactions without further purification.

4.2.3 Computational methods. All the calculations were performed *in vacuo* using the Gaussian 16 program package.[28] Optimizations were performed with the B3LYP functional in conjunction with the 6-31G(d) basis set.[30] The reaction pathways were confirmed by IRC analyses performed at the same level calculations. Vibrational frequencies were computed at the same level of theory to define the optimized structures as minima or transition states, all of which present an imaginary frequency corresponding to the forming bonds.

4.2.4 Synthesis of CS and CS-POSS 7 hydrogels. Chitosan powder with medium molecular weight (240 mg) or the hybrid sample CS-POSS 7 was dispersed in an aqueous solution of 2% acetic acid at 45 °C, for 30 min. Then, the cross-linking agent genipin (24 mg, 0.1 mmol) was slowly added to the mixture. The so formed hydrogels were rinsed with deionized water and stored in a hermetic sealed pan at the temperature of 15 °C at a constant relative humidity by adding a beaker containing water inside the hermetically sealed pan. The formulations were periodically weighed to verify that no loss of water occurred. For measuring the water content and then, the final wt% of the composite, the hydrogels were dried in a baker at 37 °C for 24 hours at the vacuum drying pressure of 65 mbar, up to constant weight. The amount of water was evaluated as difference between the weight of composite before and after drying and was found to be of 94 wt% and 78 wt% for CS and CS-POSS 7 hydrogels, respectively.

4.2.5 Synthesis of ketoprofen-doped samples. Chitosan powder with medium molecular weight (240 mg) or the CS-POSS 7 sample (240 mg), was dispersed in an aqueous solution of 2% acetic acid at 45 °C, for 30 min. Then, ketoprofen lysine salt (160 mg, 0.67 mmol) dissolved in 2 mL of deionized water and subsequently, the cross-linking agent genipin (24 mg, 0.1 mmol) were slowly added to the mixture. The formed hydrogels were rinsed with deionized water and dried at 37 °C for 24 h at the vacuum drying pressure of 65 mbar and then used for the subsequent drug release studies.

4.2.6 Drug release studies. The ketoprofen release from CS and CS-POSS 7 hydrogels was performed using a phosphate buffered saline solution (PBS) at pH 7.4 and at the temperature of 37 °C, using a dialysis bag diffusion technique. In a typical experiment, 800 mg of sample, sealed in dialysis bag was immersed in 40 mL of PBS in a beaker under slow speed magnetic stirring, then, 3 mL of sample was withdrawn periodically and after each measurement the same aliquot was added back to the release system. The amount of ketoprofen released in buffer was quantified by UV-Vis absorption spectra by measuring the absorbance at 260 nm relative to a calibration curve recorded under the same conditions.

4.2.7 Biological studies. To assess the cytotoxicity of CS and CS-POSS 7 hydrogels were used the human fetal osteoblastic cell line (hFOB 1.19 cells). The cells were cultured in a 1 : 1 mixture of Dulbecco's Modified Eagle's Medium/

Nutrient Mixture F-12 Ham with L-glutamine (2.5 mM), sodium pyruvate (0.5 mM), sodium bicarbonate (1.2 g L^{-1}), G418 (0.3 mg mL^{-1}) and fetal calf serum (10%). We used exposure concentrations ranging from 0.3 to 1.5 mg mL^{-1} for CS hydrogel and CS-POSS 7 hydrogel (see ESI†) that were stratified in a 12 multi-well plate, forming drops which were gelified at room temperature. In each well the surface covered by the nanosystems was calculated by means the Image J software. Hence, the plates were sterilized through a 24 h UV radiation treatment and then the cells were plated (approximately 3×10^5 cells per well) and grown for 48 h at 34 °C in an atmosphere of 5% CO_2. In each experiment, we included monolayers grown in the absence of compounds as negative controls (*i.e.* control cells). Since the interference of compounds did not make it possible to perform the formazan-based colorimetric viability test, we labelled hFOB 1.19 cells with the DNA intercalating probe propidium iodine (PI) in order to evaluate cytotoxicity. Briefly, after the growth of the monolayers for the experimental times with and without the examined compounds, suspensions formed by detached cells were loaded with propidium iodine (3 mg mL^{-1}) and counted. The mortality rate was assessed by fluorimetric analysis (λ_{exc} 493–λ_{em} 636 nm). The emission values recorded in treated cells were compared with control cells whose cell mortality rate was 5%. To quantify the viable cells, we fixed and permeabilized the adherent cells with cold 70% ethanol for 30 min at 4 °C, and then we stained with propidium iodine (3 mg mL^{-1}). By using the same wavelengths above reported, the values were recorded by using a microtiter plate reader (Tecan Italia, Milan-Italy). The biological tests were all performed in triplicate, and the replicates were calculated as means ± SD comparing the obtained values in exposed cells with those obtained by the negative control. In addition, to evaluate cell morphology and the lysosomal compartment, the adherent treated and untreated cells were also labelled with the metachromatic fluorophore Acridine Orange (AO) and confocal observations were performed (CLSM, TCS-SP2, Leica-Microsystems, Germany).

Conflicts of interest

There are no conflicts to declare.

Acknowledgements

We gratefully acknowledge the Universities of Catania and Messina, Interuniversity Research Centre on Pericyclic Reactions and Synthesis of Hetero and Carbocycles Systems and the Interuniversity Consortium for Innovative Methodologies and Processes for Synthesis (CINMPIS) for partial financial support. The authors are very grateful to Professor Pierluigi Caramella for helpful discussion and suggestions.

References

1 S.-B. Park, E. Lih, K.-S. Park, Y. K. Joung and D. K. Han, *Prog. Polym. Sci.*, 2017, **68**, 77–105.
2 Y. Zhang, X. Liu, L. Zeng, J. Zhang, J. Zuo, J. Zou, J. Ding and X. Chen, *Adv. Funct. Mater.*, 2019, **29**, 1903279.
3 K. Zhang, S. Wang, C. Zhou, L. Cheng, X. Gao, X. Xie, J. Sun, H. Wang, M. D. Weir, M. A. Reynolds, N. Zhang, Y. Bai and H. H. K. Xu, *Bone Res.*, 2018, **6**, 31.
4 K. Farbod, M. R. Nejadnik, J. A. Jansen and S. C. G. Leeuwenburgh, *Tissue Eng., Part B*, 2013, **20**, 173–188.
5 L. Roseti, V. Parisi, M. Petretta, C. Cavallo, G. Desando, I. Bartolotti and B. Grigolo, *Mater. Sci. Eng., C*, 2017, **78**, 1246–1262.
6 R. Song, M. Murphy, C. Li, K. Ting, C. Soo and Z. Zheng, *Drug Des., Dev. Ther.*, 2018, **12**, 3117–3145.
7 S. Tiwari, R. Patil and P. Bahadur, *Polymers*, 2019, **11**, 1–23.
8 K. M. Galler, R. N. D'Souza and J. D. Hartgerink, *J. Mater. Chem.*, 2010, **20**, 8730–8746.
9 M. Rodríguez-Vázquez, B. Vega-Ruiz, R. Ramos-Zúñiga, D. A. Saldaña-Koppel and L. F. Quiñones-Olvera, *BioMed Res. Int.*, 2015, 1–15.
10 F. Croisier and C. Jérôme, *Eur. Polym. J.*, 2013, **49**, 780–792.
11 R. LogithKumar, A. KeshavNarayan, S. Dhivya, A. Chawla, S. Saravanan and N. Selvamurugan, *Carbohydr. Polym.*, 2016, **151**, 172–188.
12 S. Gao, G. Tang, D. Hua, R. Xiong, J. Han, S. Jiang, Q. Zhang and C. Huang, *J. Mater. Chem. B*, 2019, **7**, 709–729.
13 S. Deepthi, J. Venkatesan, S.-K. Kim, J. D. Bumgardner and R. Jayakumar, *Int. J. Biol. Macromol.*, 2016, **93**, 1338–1353.
14 K. C. Kavya, R. Jayakumar and S. K. P. Chennazhi, *Int. J. Biol. Macromol.*, 2013, **59**, 255–263.
15 (*a*) A. Pistone, D. Iannazzo, C. Celesti, E. Piperopoulos, D. Ashok, A. Cembran, A. Tricoli and D. Nisbet, *Materials*, 2019, **12**, 2321; (*b*) A. Pistone, D. Iannazzo, S. Galvagno, C. Espro, A. Tampieri, m. Montesi, S. Panseri and M. Sandri, *Engineering*, 2017, **3**(1), 55–59.
16 Y. Yu, Z. Bacsik and M. Edén, *Materials*, 2018, **11**, 1–18.
17 D. B. Cordes, P. D. Lickiss and F. Rataboul, *Chem. Rev.*, 2010, **110**, 2081–2173.
18 S. Tamburaci and F. Tihminlioglu, *J. Mater. Sci.: Mater. Med.*, 2018, **29**, 1–15.
19 S. L. Chew, K. Wang, S. P. Chai and K. L. Goh, *J. Mater. Sci.: Mater. Med.*, 2011, **22**, 1365–1374.
20 Y. Zhang, M. Chen, J. Tian, P. Gu, H. Cao, X. Fan and W. Zhang, *Biomater. Sci.*, 2019, **7**, 3266–3276.
21 H. Ghanbari, B. G. Cousins and A. M. Seifalian, *Macromol. Rapid Commun.*, 2011, **32**, 1032–1046.
22 S. L. Chew, K. Wang, S. P. Chai and K. L. Goh, *J. Mater. Sci.: Mater. Med.*, 2011, **22**, 1365–1374.
23 Y.-M. Ha, T. Amna, M.-H. Kim, H.-C. Kim, M. S. Hassan and M.-S. Khil, *Colloids Surf., B*, 2013, **102**, 795–802.
24 (*a*) U. Chiacchio, A. Padwa and G. Romeo, *Curr. Org. Chem.*, 2009, **13**, 422–447; (*b*) R. Romeo, C. Carnovale, S. V. Giofrè, M. A. Chiacchio, A. Garozzo, E. Amata, G. Romeo and U. Chiacchio, *Beilstein J. Org. Chem.*, 2015, **11**, 328–334; (*c*) S. V. Giofrè, R. Romeo, C. Carnovale, R. Mancuso, S. Cirmi, M. Navarra, A. Garozzo and M. A. Chiacchio, *Molecules*, 2015, **20**, 5260–5275; (*d*) F. P. Ballistreri, C. M. A. Gangemi, A. Pappalardo, G. A. Tomaselli, R. M. Toscano and G. Trusso Sfrazzetto, *Int. J. Mol. Sci.*, 2016, **17**, 1112; (*e*)

A. Brandi, F. Cardona, S. Cicchi, M. Cordero and A. Goti, *Org. React.*, 2017, **94**, 1–321; (*f*) I. Blanco, L. Abate, P. Bottino and M. A. Chiacchio, *J. Therm. Anal. Calorim.*, 2018, **134**, 1337–1344; (*g*) L. Abate, F. A. Bottino, G. Cicala, M. A. Chiacchio, G. Ognibene and I. Blanco, *Polymers*, 2019, **11**, 1475; (*h*) M. A. Chiacchio, L. Legnani, A. Campisi, P. Bottino, G. Lanza, D. Iannazzo, L. Veltri, S. Giofré and R. Romeo, *Org. Biomol. Chem.*, 2019, **17**, 4892–4905; (*i*) S.-I. Murashi and Y. Imada, *Chem. Rev.*, 2019, **119**, 4684–4716; (*j*) A. I. Said and T. I. El-Emary, *RSC Adv.*, 2020, **10**, 845–850.

25 C. C. Tsai, R. N. Huang, H. W. Sung and H. C. Liang, *J. Biomed. Mater. Res.*, 2000, **52**, 58–65.

26 M. A. Chiacchio, l. Borrello, G. Di Pasquale, A. Pollicino, F. A. Bottino and A. Rescifina, *Tetrahedron*, 2005, **61**, 7986–7993.

27 (*a*) L. Legnani, L. Toma, M. A. Chiacchio, S. Giofré, I. Delso, T. Tejero and P. Merino, *J. Org. Chem.*, 2016, **81**, 7733–7740; (*b*) M. A. Chiacchio, L. Legnani, P. Caramella, T. Tejero and P. Merino, *Eur. J. Org. Chem.*, 2017, 1952–1960; (*c*) P. Merino, M. A. Chiacchio, L. Legnani, I. Delso and T. Tejero, *Org. Chem. Front.*, 2017, **4**, 1541–1554; (*d*) M. A. Chiacchio, L. Legnani, P. Caramella, T. Tejero and P. Merino, *Tetrahedron*, 2018, **74**, 5627–5634; (*e*) L. Legnani, R. Puglisi, A. Pappalardo, M. A. Chiacchio and G. Trusso Sfrazzetto, *Chem. Commun.*, 2020, **56**, 539–542.

28 M. J. Frisch, G. W. Trucks, H. B. Schlegel, G. E. Scuseria, M. A. Robb, J. R. Cheeseman, G. Scalmani, V. Barone, G. A. Petersson, H. Nakatsuji, X. Li, M. Caricato, A. V. Marenich, J. Bloino, B. G. Janesko, R. Gomperts, B. Mennucci, H. P. Hratchian, J. V. Ortiz, A. F. Izmaylov, J. L. Sonnenberg, D. Williams-Young, F. Ding, F. Lipparini, F. Egidi, J. Goings, B. Peng, A. Petrone, T. Henderson, D. Ranasinghe, V. G. Zakrzewski, J. Gao, N. Rega, G. Zheng, W. Liang, M. Hada, M. Ehara, K. Toyota, R. Fukuda, J. Hasegawa, M. Ishida, T. Nakajima, Y. Honda, O. Kitao, H. Nakai, T. Vreven, K. Throssell, J. A. Montgomery Jr, J. E. Peralta, F. Ogliaro, M. J. Bearpark, J. J. Heyd, E. N. Brothers, K. N. Kudin, V. N. Staroverov, T. A. Keith, R. Kobayashi, J. Normand, K. Raghavachari, A. P. Rendell, J. C. Burant, S. S. Iyengar, J. Tomasi, M. Cossi, J. M. Millam, M. Klene, C. Adamo, R. Cammi, J. W. Ochterski, R. L. Martin, K. Morokuma, O. Farkas, J. B. Foresman, and D. J. Fox, *Gaussian 16, Revision C.01*, Gaussian, Inc., Wallingford CT, 2016.

29 B. R. Kim, H. G. Lee, S. B. Kang, G. H. Sung, J. J. Kim, J. K. Park, S. G. Lee and Y. J. Yoon, *Synthesis*, 2012, **1**, 42–50.

30 (*a*) A. D. Becke, *J. Chem. Phys.*, 1993, **98**, 5648–5652; (*b*) C. Lee, W. Yang and R. G. Parr, *Phys. Rev. B: Condens. Matter Mater. Phys.*, 1988, **37**, 785–789.